

Evidence of the influence of reflections on the Z_{eff} profile measurements and their mitigation

B. Schunke, G. Huysmans, P. Thomas

Association Euratom-CEA sur la Fusion Contrôlée, CEA Cadarache, 13108 St-Paul-Lez-Durance, France.

1. Introduction

There is a significant interest in the reconstruction of a Z_{eff} profile to assess the control of the plasma impurities. On Tore Supra (TS) a modified Abel inversion [1] of the visible bremsstrahlung allows to calculate the Z_{eff} profile. Although the total number of viewing lines of the bremsstrahlung diagnostic is small, the method gives acceptable accuracy due to the high poloidal symmetry (circularity) of the TS plasma. It had been noticed that the outer channels were often over-estimated, giving unphysically high Z_{eff} values at the edge of 20 or more. Ideally in the case of a derived parameter like the Z_{eff} , the parameters used in the calculation, such as n_e and T_e profiles, should be measured in the same toroidal location and the same poloidal plane as the bremsstrahlung. This is not possible due to access problems, and so introduces errors but not on the scale of those observed in the profile reconstruction. The Abel inversion itself, although very sensitive to noise and errors in the measurements, is also unlikely to introduce the observed over-estimation of the outer channels.

2. Experimental set-up

On TS, the mean effective charge Z_{eff} of the plasma is extracted from line integrated measurements of visible bremsstrahlung, following the approach by Kadota [2]. The visible Bremsstrahlung is observed using a fan of 12 poloidal viewing lines (Fig. 1) in a narrow wavelength interval, observing a well defined, restricted plasma volume [3]. The detection system consists of a telescope, which focuses the incoming light onto the 12 optical fibres mounted in a single array, an optical interference filter and an acquisition system consisting of photomultipliers (PMs) operated in counting mode, a VME ICV102 card, and the central TS data storage system. The central wavelength of the interference filter is 523.8nm with a spectral bandwidth of 1nm, which corresponds to the impurity-line free region in TS. All fibres end in individual PMs and acquisition channels. An independent toroidal viewing line observes the bremsstrahlung through a different window, thus allowing reference measurements. In 2003 a further poloidal sightline was available, connected to a miniature large path band (LPB) spectrometer (OceanOptics ST2000).

Preliminary observations, with both a high-resolution spectrometer and the LPB spectrometer, indicated that there is no systematic line radiation in the wavelength interval observed and the background follows the $1/\lambda$ dependency of bremsstrahlung. Therefore a series of dedicated discharges were carried out, during which the plasma was pushed onto the limiter and the radius was varied so that the outer channels of the diagnostic were outside the plasma at several times during the discharge (Fig. 1). However, the outer channels still measured a signal even when the viewing cord was not passing the plasma (Fig. 2). This led to the conclusion that reflections on the vacuum vessel wall were responsible for the additional signal component and it was attempted to model their influence on the calculated profile.

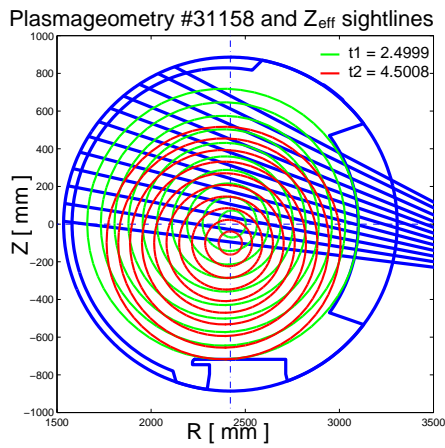


Figure 1: Flux surfaces of the dedicated discharge and diagnostic viewing lines

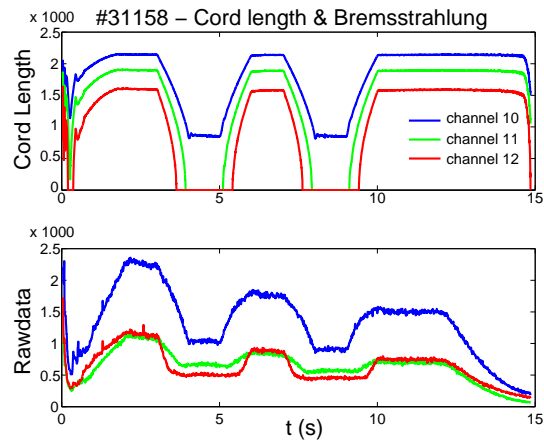


Figure 2: Cord length of the last 3 edge channels and their photomultiplier signals

3. Reflection modelling

The reflection model is expressed in the so-called bidirectional reflectance distribution function (BRDF), defined as the ratio between the incoming irradiance and the outgoing radiance [4]. Several models, with increasing complexity, were considered. For Lambertian diffusion, the BRDF is a constant, independent of the incoming and outgoing directions, expressed using a reflection coefficient, $BRDF = R_{diff} / \pi$. The simplest model for specular reflection, the Phong model, considers a cosine dependency: $BRDF = R_{spec} (\cos \theta)^p$, with θ the angle between the telescope and the reflection vector, R_{spec} the specular reflection parameter and p a material constant. A more elaborate model, known as the Blinn-Cook-Torrance (BCT) model, is based on the reflection of a rough surface made out of micro-facets with a certain distribution, $BRDF = \frac{R_{bct}}{\pi} DG((-\vec{n} \cdot \vec{c})(\vec{n} \cdot \vec{s}))^{-1}$, where

$D = (4m^2 \cos^4 \gamma)^{-1} e^{-((\tan \gamma)/m)^2}$ is the Beckmann distribution function describing the surface roughness, and the factor G describing the masking and shadowing among the microfacets. To compare the 3 models, the reflected signal is calculated for each of the 12 channels coming from a plasma assuming constant emission. The plasma is shifted down such that channels 11 and 12 do not cross the plasma (similar to discharge #31158 at 4.9s).

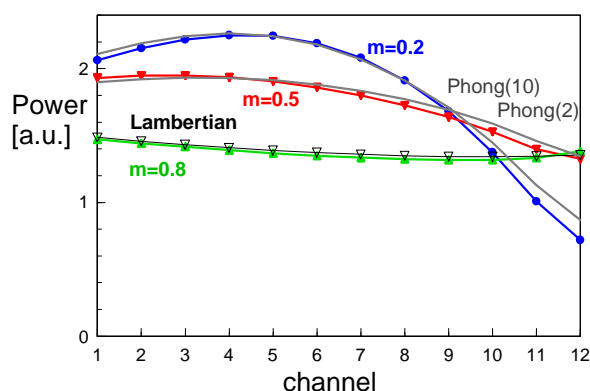


Figure 3 Comparison of the different reflection models

reflections to the higher channels is significantly lower than for the channels closer to the mid-plane. This can be understood from the angle between the wall-normal and the line-of-sight, which increases with channel number. As a consequence, the higher channels see less of the plasma in the reflected signal. This is visualised in Figure 4, which shows in a the origin of the reflected signal for highly specular reflection ($m=0.2$) calculated with the BCT model and compares this to the solution obtained for the diffusive case (Lambert). The choice of model depends therefore on the reflectivity of the vacuum wall of TS.

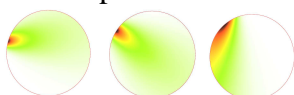


Figure 4a Origin of the reflected signal for channels 1, 5 and 12, **BCT model**, $m=0.2$)



Figure 4b Origin of the reflected signal for channels 1, 5 and 12, **Lambert**

4. Profile reconstruction

The contributions from the reflections on the wall to the measured signal should be taken into account when the measurements are inverted to produce a radiation (or Z effective) profile. This can be done by decomposing the radiation from the plasma in a set of radial basis functions (for example a set of B-splines as a function of a flux surface coordinate). For each function the direct contribution of the plasma radiation (a line integral) and the reflected contribution (a volume integral) is calculated, assuming a certain reflection model. This yields an over-determined system of equations for the unknown expansion coefficients.

The system can be solved using Singular Value Decomposition in combination with Tikhonov regularization [5]. The Tikhonov regularization parameter is determined using the L-curve method.

To show the influence of the reflections on the reconstructed profiles, synthetic data based on a flat Zeff profile, including the contribution from diffuse (Lambertian) reflections with a 25% reflection coefficient, a reasonable value for the inner wall panels in TS, have been

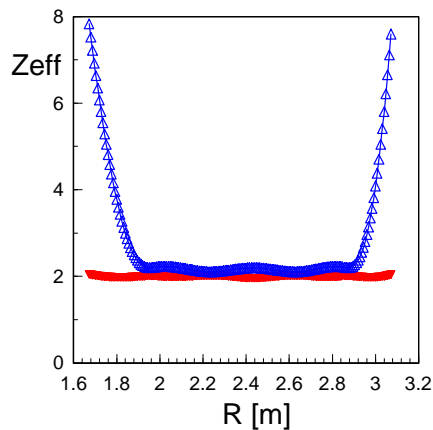


Figure 4a Profile reconstruction with and without reflections

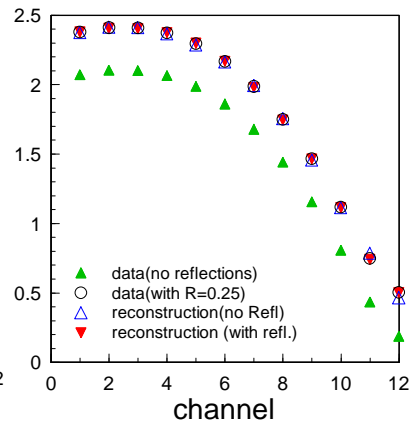


Figure 4b Synthetic data reconstructed data

used as input for the reconstruction.

Figure 4a compares the profiles resulting from the inversion with (red) and without (blue) taking the reflections into account. Neglecting

the reflections leads to a large overestimation of the Zeff values close to the plasma boundary. Figure 4b shows the synthetic data and the reconstructed data after the fit.

5. Conclusions

The contributions of reflections to the Z_{eff} diagnostics in the present configuration of TS has been investigated using dedicated discharges. An inversion method has been developed demonstrating that the presence of reflections leads to an over-estimation of the outer channels in the reconstruction of the Z_{eff} profile. To evaluate which model best describes the reflections present in TS the exact value of the reflection coefficient has to be determined. Further investigation of the reflection coefficient is under way.

References

- [1] J. Blum, et. al. Nucl. Fusion **30** (1990) 1475
- [2] K. Kadota, et. al., Nucl. Fus. **20**, (1980) 209
- [3] B. Schunke, et. al. J. Nucl. Materials, **290-293**, (2001) 715
- [4] L. Neumann, et. al., Eurographics **18** (1999)
- [5] P.C. Hansen, 'The L-curve and its use in the numerical treatment of inverse problems' Computational Inverse Problems in Electrocadiology' WIT Press Southampton 2001 (<http://citeseer.ist.psu.edu/393521.html>)